Journal of CO2 Utilization 93 (2025) 103053

Contents lists available at ScienceDirect

Journal of CO2 Utilization

journal homepage: www.elsevier.com/locate/jcou

Coupling Ni-based anodes for textile industry process stream electrooxidation with electrocatalytic CO_2 reduction to formate in gas phase

Jose Antonio Abarca [a], Ghazaleh Abdolhosseini [b], Juan Marcos Sanz [c], Jose Solla-Gullón [d,*], Felipe A. Garcés-Pineda [b], Guillermo Díaz-Sainz [a], Angel Irabien [a]

[a] Departamento de Ingenierías Química y Biomolecular, Universidad de Cantabria, Avenida de los Castros s/n, Santander 39005, Spain
[b] Institute of Chemical Research of Catalonia (ICIQ), The Barcelona Institute of Science and Technology (BIST), Av. Països Catalans 16, Tarragona 43007, Spain
[c] Textil Santanderina, S.A., R+D Department, Avenida Textil Santanderina s/n, Cabezón de la Sal, 39500, Spain
[d] Institute of Electrochemistry, University of Alicante, Apdo. 99, Alicante 03080, Spain

ARTICLE INFO

Keywords:
Gas-phase CO_2 electroreduction
Ni-based anodes
OER
Textile industry streams oxidation
Formate

ABSTRACT

Scaling up CO_2 electroreduction to formate faces several challenges, including using chemicals as electrolytes and high energy demands. To address these issues, this study uses an industrial stream—specifically a caustic soda stream from the textile industry—as anolytes for the oxygen evolution reaction (OER). Using this approach, formate concentrations of 226 g L^{-1} and Faradaic efficiencies (FE) of 53 % are achieved at 200 mA cm^{-2}, demonstrating the competitiveness of industrial streams compared to synthetic anolyte solutions. Various anode materials are tested to optimize OER kinetics under industrial conditions and reduce energy consumption. Ni foam exhibited promising results, achieving FEs of 78 % and 58 % at 90 and 200 mA cm^{-2}, with energy consumption between 236 and 385 kWh $kmol^{-1}$, making it one of the most efficient options among commercially available materials. In addition, alternative materials, such as NiFeOx and NiZnFeOx particulate anodes, are synthesized to provide viable substitutes for commercial anodes that rely on scarce elements. These alternatives demonstrated similar formate concentrations, with FEs up to 74 % and reduced energy requirements compared to commercial NiO. The synthesized NiFe foam anode excelled in performance, with energy consumption below 210 and 380 kWh $kmol^{-1}$ and an impressive formate production of 255 g L^{-1} of formate achieving a 60 % FE at 200 mA cm^{-2}. Overall, this research demonstrates the feasibility of CO_2 electroreduction to formate using textile effluents under relevant conditions, representing a significant step toward making this process a competitive option for decarbonizing hard-to-abate industries.

1. Introduction

The extensive use of fossil fuels for industrial development over the past century has led to a significant and exponential increase in atmospheric CO_2 levels. Current CO_2 concentrations have reached 425 ppm, nearly double the levels of the preindustrial era [1]. This rapid rise in CO_2 is a primary driver of global warming and climate change. To mitigate the long-term impacts of climate change, various international agreements have proposed strategies to reduce and minimize CO_2 emissions [2]. Key strategies include transitioning to renewable energy sources, decarbonizing the energy sector, and electrifying industrial processes [3]. However, not all economic sectors can easily reduce CO_2 emissions through conventional methods. The so-called “hard-to-abate” sectors refer to industries where CO_2 emissions are an intrinsic part of the production process, making decarbonization particularly challenging. To address these emissions, alternative approaches are necessary. In this context, Carbon Capture and Utilization (CCU) strategies have emerged as promising technologies [4,5]. These strategies not only prevent the direct release of CO_2 into the atmosphere but also enable the recycling of captured CO_2 to produce valuable products.

Among the different utilization technologies, CO_2 electroreduction to value-added products is particularly promising [6], as it allows excess energy from renewable energy sources to be stored in chemical bonds [7]. A wide range of CO_2 reduction products can be obtained through

* Corresponding author.
E-mail address: jose.solla@ua.es (J. Solla-Gullón).

https://doi.org/10.1016/j.jcou.2025.103053
Received 11 December 2024; Received in revised form 6 February 2025; Accepted 26 February 2025
Available online 28 February 2025
2212-9820/© 2025 The Author(s). Published by Elsevier Ltd. This is an open access article under the CC BY-NC-ND license (http://creativecommons.org/licenses/by-nc-nd/4.0/).

this process, including formate/formic acid, methanol, ethanol, methane, or ethylene, among others, by applying an external potential to an electrochemical cell [8–10]. Formate is especially noteworthy as a reduction product, being among the most advanced chemicals in terms of CO_2 electrochemical reduction at an industrial scale [11]. However, further research is needed, as the Technology Readiness Level (TRL) currently stands between 4 and 5, with early prototypes still needing to operate in industrial environments.

The core component of CO_2 electroreduction technology is the electrochemical reactor, which consists of two separate electrodes [11]. Among the different reactor configurations, gas-phase operation has shown significant potential for scalability. In this configuration, reactants pass through the reactor in a single pass, achieving high formate concentrations and approaching the industrial target of 85 % wt. formate production via CO_2 recycling [12]. Here, the cathode feed consists of humidified CO_2, while the anolyte is in the liquid phase. The CO_2 reduction reaction takes place at the three-phase boundary (gas--liquid-solid), which includes the gaseous CO_2, the humidity from the feed stream, and the catalyst surface [13]. An ion exchange membrane separates the cathode and anode compartments, allowing charged species to flow between the electrodes depending on the membrane type [14]. Cation exchange membranes (CEM) are primarily used in CO_2 electroreduction to formate, as they allow protons from the anode to cross and participate in the reduction reaction while preventing the migration of formate anions to the anode, where they could be re-oxidized [15]. Finally, an oxidation reaction occurs at the anode, and the electrons generated are directed to the cathode via an external electrical circuit to support the CO_2 reduction reaction.

Different synthetic anolytes are used to carry out the oxidation reaction at the anode. The Oxygen Evolution Reaction (OER) is the most common oxidation process paired with CO_2 electroreduction at the laboratory scale. However, other oxidation reactions coupled with the CO_2 electroreduction, such as ethanol [16], methanol [17,18], or methyl orange [19,20] oxidations in addition to Glycerol Oxidation Reaction (GOR) [21,22], are also being explored for their potential benefits. In this regard, very recently, Xie at al. [23] have exhaustively revised some alternative oxidation reactions to replace the OER and reduce energy consumption at the anode while producing higher-value chemicals. Alkaline solutions are frequently used at the anode to promote CO_2 reduction to formate while suppressing competing reactions like the Hydrogen Evolution Reaction (HER) [24]. Common supporting electrolytes in these solutions include KOH, $KHCO_3$, and K_2SO_4 [11]. Alkaline hydroxides, in particular, are preferred because they enhance CO_2 electroreduction kinetics, achieving higher current densities than neutral anolytes such as $KHCO_3$ or K_2SO_4 under the same applied potential [25]. In some approaches, acidic anolytes are used to improve system stability, although they tend to favor HER, which can reduce the efficiency of CO_2 reduction to formate [26].

To assess the technical feasibility of scaling this technology for industrial applications, it is essential to evaluate the use of industrial streams as sources for oxidation reactions [27]. Exploring the potential of such process streams, particularly when aligned with relevant oxidation reactions, could lower overall costs and advance circular economy principles in industrial settings [28].

This study investigates the feasibility of installing a CO_2 recycling plant in a hard-to-abate sector, specifically within the textile industry, which represents an intensive CO_2-emission sector [29]. Besides, formic acid/formate is employed as a chemical for wastewater treatment in this industry. It evaluates various industrial streams from different textile processes as potential anolytes for oxidation reactions coupled with CO_2 electroreduction to formate [30]. Among the examined textile processes, mercerization appears to be the most compatible for integration with CO_2 electroreduction [31,32]. In this process, cotton fabric is treated with highly concentrated sodium hydroxide (NaOH) [32]. As previously mentioned, alkaline hydroxides are particularly advantageous for coupling with CO_2 electroreduction to formate. Process streams can be sourced from different stages of mercerization, either from the inlet, where NaOH is highly concentrated after a recovery stage, or from the outlet, where NaOH is diluted with tap water. Another textile process that may provide suitable effluent for anolytes is the causticizing process, in which cotton fabric is treated with less concentrated NaOH that does not undergo a recovery stage but retains high purity [31]. This study experimentally evaluates the technical feasibility of using process streams from both operations as viable anolytes.

The OER, typically paired with CO_2 electroreduction, has been extensively studied using noble metals as catalysts [11,33]. Platinum (Pt) and Iridium (Ir)-based materials demonstrate high activity across a broad pH range. However, the scarcity and high cost of these materials highlight the need for alternative, non-precious metals alternatives that can perform the OER [34]. Nickel (Ni), an earth-abundant first-row transition metal, has been known as an OER catalyst since the early 20th century [35] and has recently emerged as an efficient and cost-effective alternative in water-splitting applications due to its low price, availability, and high OER activity, especially in alkaline media [36–38]. Ni also serves as the primary catalyst in commercial alkaline water electrolyzers [39]. Several works have employed Ni-based materials as counter electrodes in CO_2 electroreduction to formate using various anode morphologies, from particulate anodes [38] to commercial Ni foams [40], to achieve high current densities. These configurations improve mass transfer and provide a large active surface area, enhancing electronic conduction compared to conventional plate anodes.

Other transition metals, such as Iron (Fe) or Zinc (Zn), are also considered effective OER catalysts, although their use with CO_2 electroreduction to formate has been limited. Nevertheless, Fe and Zn show promising OER performance in alkaline conditions, making them potential candidates for coupling with CO_2 electroreduction [41]. Experimental studies reveal that Ni-oxyhydroxide evolves during operation by incorporating Fe from the electrolyte, resulting in a highly active Fe-doped Ni OER catalyst [42,43]. In addition, Zn-doped hematite [44] and Zn-doped spinel (AB_2O_4) have been proposed as promising alternatives, lowering overpotentials and enabling new reaction pathways through cooperative push-pull interactions among Ni-Fe-Zn centers on the catalyst surface [45]. Furthermore, the incorporation of phosphorous into the crystalline structure of certain NiFe catalysts has been explored, demonstrating exceptional OER performance in alkaline media, and indicating their potential for near-industrial applications [35].

Hence, the primary objective of this work is to explore the feasibility of using textile industry streams as electrolytes for continuous CO_2 electroreduction to formate in gas phase, a novel approach with limited coverage in current literature, making this work a significant advancement in CO_2 electroreduction under industrial conditions. Specifically, textile industry streams are collected, characterized, and tested as anolytes in an electrochemical cell. To enhance the OER at the anode, various anodic materials are studied, including commercial Ir-based DSA plates and synthesized Ni-based anodes combined with other non-precious materials. These materials are characterized and tested to assess their electrocatalytic activity. The CO_2 electroreduction experiments are conducted in a laboratory set-up, using different anodic materials and morphologies, such as plates, foams, and particulate anodes. The system's performance is evaluated based on key metrics, including Faradaic Efficiency (FE), formate production rate, energy consumption, and overall energy efficiency. The findings from this study represent a significant step forward in implementing CO_2 electroreduction to formate within industrial environments.

2. Methodology

2.1. Textile industry stream characterization

Textile industry streams are collected from four different points

across two textile processes. From the mercerization process, samples are taken from both the inlet and outlet of the mercerizing machine. Caustic soda mercerizing is the most widely used technique for cotton, where fabric is treated under tension in a concentrated caustic soda solution (270 – 300 g NaOH/l, or 170 – 350 g NaOH/kg) for approximately 40–50 seconds. The same equipment is utilized for desizing and caustification, which involve a combination of desizing and cold bleaching. In these processes, the fabric is immersed in a bath containing hydrogen peroxide, caustic soda, stabilizers for hydrogen peroxide, and complexing agents, with persulphate commonly added to the solution. Here, caustic soda is applied at a lower concentration (145 – 190 g/l) without tension, allowing the fabric to shrink and thus improving dye absorption. Beyond its desizing and bleaching effects, this treatment also serves as a pre-scouring process. After the reaction, the fabric is thoroughly rinsed with hot water (95 ºC) [46].

During both the mercerizing and caustification processes, a first sample is collected in the initial phase, exhibiting a pH range of 12–13, while a second stream is taken post-wash, where pH values are slightly lower (10−12). Considerations must be made for suspended particles and residual washing agents.

The collected textile industry streams are then characterized to assess their potential as anolytes for CO_2 electroreduction to formate. A full physicochemical characterization includes measurements of pH (pHmeter Violab pH 50, XSinstruments), conductivity (Crinson CM35 +), composition, determined by ion chromatography (Dionex ICS-5000 for anion and cation detection, AS9 column and Na_2CO_3 as eluent for anion determination and CS12 column and CH_4SO_3 as eluent for cation detection), as well as total and suspended solids (Following the UNE 77034). The dissolved solids are determined by subtracting the suspended solids from the total solids. Parameters such as conductivity and pH are critical for determining the electrolyte behavior in the CO_2 electroreduction reaction, where maximizing selectivity depends on these properties.

2.2. Anode materials

Different anode materials are employed to carry out the OER reaction using the textile industry streams as anolytes. Initial tests use commercial anodes to assess the viability of coupling each stream's oxidation; three materials are proposed. The benchmark, a dimensionally stable anode, DSA/O_2 (Ir-MMO mixed metal oxide on platinum), is widely employed in previous studies [12,26,33]. Another approach utilizes commercial NiO nanoparticles (Sigma Aldrich, 50 nm) coated on carbon paper (Toray TGP-H-60) to form a particulate anode, with a loading of 1.5 mg cm^{-2} and Nafion (D-521, Ion Power) as a binder. This setup has demonstrated high performance in OER coupled with CO_2 reduction to formate [38]. A commercial Nickel foam (Racemat CV, Niquel foam Grade 4753 thickness 1.6 mm) is also evaluated as an alternative configuration.

Following tests with commercial anodes, synthesized nanoparticles are used to fabricate particulate anodes aimed at improving the OER. $NiFeO_x$ and $NiZnFeO_x$ are synthesized via a hydrothermal method, using equimolar metal nitrates are dissolved in water (metal concentration: 50 mM), then hydrolyzed with diluted aqueous ammonia to achieve pH 8.5. The solution is placed in a Teflon cup in an autoclave at 140 °C for 2 hours. After hydrothermal treatment, the pressure vessel is air-cooled, and the product is washed with water (H_2O) and ethanol (CH_3CH_2OH), with nanoparticles collected by centrifugation (final particle size: ~8 nm).

To decorate Ni foam electrodes with Fe-Ni oxyhydroxide nanostructured, a modified multi-step process is employed based on previous methods [35]. First, a piece of commercial Ni foam (0.5 mm) is dipped into an iron nitrate solution (prepared by dissolving 7.5 g Fe $(NO_3)_3 \cdot 9\ H_2O$ precursor in 50 mL deionized water) and slowly dried in air. After drying, it is thermally phosphatized in a tube furnace at 450°C. The phosphorus source was 600 mg sodium hypophosphite monohydrate ($NaH_2PO_2 \cdot H_2O$), which is put upstream of the Ar circulation at around 400°C. This thermal phosphidation forms $Fe(PO_3)_2$ nanocrystals on top of the Ni_2P surface formed on the Ni foam, during cooling down to room temperature under argon. This immersion/-phosphidation process is repeated twice to yield a $Fe(PO_3)_2$ loading of 2–3 mg cm^{-2}.

The fabricated anodes are physically characterized using Powder X-ray diffraction, obtained with a Bruker AXS D8-Discover diffractometer (40 kV and 40 mA). Environmental scanning electron microscopy data are obtained using Quanta 600 equipment from FEI under high-vacuum conditions with a Large-Field Detector at 20 kV. Transmission electron microscopy is performed with a JEOL JEM1011 microscope operating at 80 or 100 kV, equipped with a high-contrast 2k × 2k AMT mid-mount digital camera. High-resolution transmission electron microscopy (HRTEM) and scanning transmission electron microscopy (STEM) investigations are performed on a field emission gun FEI Tecnai F20 microscope. High-angle annular dark-field (HAADF) STEM is combined with electron energy loss spectroscopy (EELS) in the Tecnai microscope using a GATAN QUANTUM energy filter to obtain compositional maps.

The morphology and particle size distribution of the Bi/C electrocatalyst are assessed using Transmission Electron Microscopy (TEM, JEOL JEM-2010 at 200 kV and JEOL JEM-1400 at 120 kV). The Bi/C GDEs are also characterized by powder X-ray diffraction (PXRD, Philips X'PERT PRO at 40 kV and 40 mA). The electrode microstructure is determined by Scanning Electron Microscopy (SEM, JEOL JSM-7000F at 10–20 kV), and the Bi distribution across the GDE is evaluated through elemental EDX mapping (SEM/EDX, HITACHI S-3000 N microscope working at 20 kV with X-ray detector Bruker Xflash).

For electrochemical double-layer capacitance (EDLC) measurements, open circuit potentials (OCPs) vs. the Hg/HgO reference electrodes are firstly recorded for 30 min to reach rather stable values. Combined with the above CV measurements, the 100 mV potential windows centered at OCPs could be determined and cyclic voltammetries are then carried out under scanning rates of 5, 10, 25, 65, 75, 90, and 100 mV s^{-1}. The current density differences between the minimum and maximum values at OCPs vs. the Hg/HgO and the corresponding scanning rates are plotted to calculate the EDLC value (1/2 of the slope of current density-scan rate plots).

2.3. Continuous CO_2 electroreduction in gas phase using the textile industry streams as anolyte

Continuous CO_2 electroreduction to formate is carried out in a filter-press electrochemical reactor (ElectroCell) which has a 10 cm^2 geometric active area, using a single pass flow of reactants. The cell is configured for gas-phase operation, as shown in Fig. 1.a. Humidified CO_2 is continuously supplied to the cathode compartment at a rate of 200 mL min^{-1}. A Gas Diffusion Electrode (GDE) serves as the cathode, composed of a commercial gas diffusion layer (GDL) (Sigracet 39 BB, Fuel Cell Store) and a catalytic layer. Carbon-supported Bi nanoparticles, previously shown to achieve excellent results [12,33,47], are used as electrocatalysts.

The GDE is fabricated by an automated spray pyrolysis technique (ND-DP Mini Ultrasonic Spray Coater, Nadetech Innovations), previously optimized [47]. The catalytic ink is formulated utilizing isopropanol (laboratory reagent grade, ≥99.5 %, Fischer Chemicals) as the solvent (97 % wt.), and Nafion ionomer (D-521, 5 % wt. dispersion, Ion Power) as the binder, with a catalyst/ionomer ratio of 70/30. The ink is sprayed onto the GDL to achieve a catalyst loading of 0.75 mg cm^{-2}. The anode and cathode compartments are separated by a cation exchange membrane (CEM), Nafion 117 (Ion Power), which is pre-activated in 1 M NaOH and positioned in close contact with the GDE surface. A leak-free Ag/AgCl 3.4 M KCl electrode, integrated into the cell within a PTFE frame in the anode compartment, serves as the reference electrode to ensure proper wetting.

In the anode compartment, the anolyte is pumped at a constant

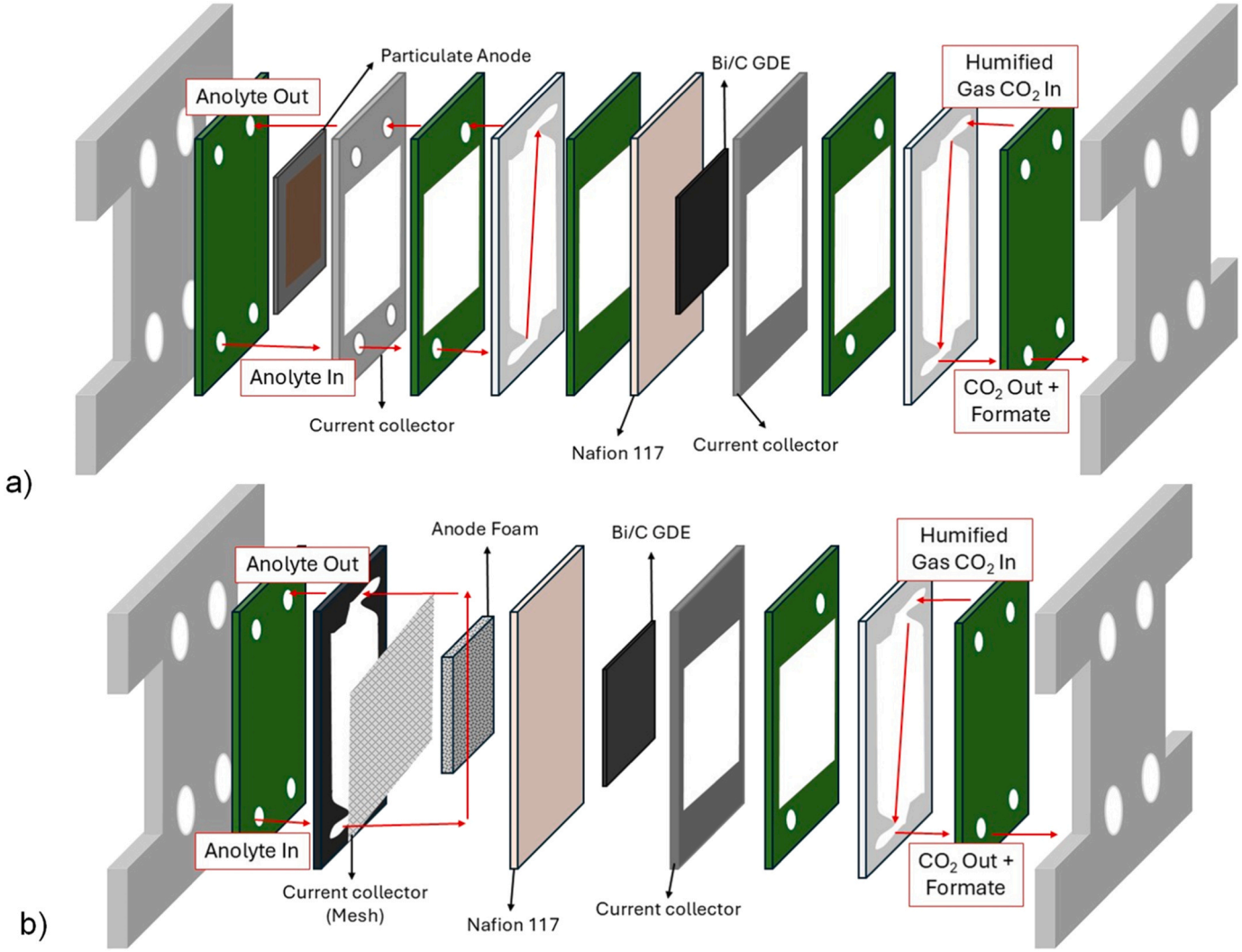

Fig. 1. Different filter-press reactor configurations when employing a) a Particulate anode and b) a Foam anode.

flowrate of 0.57 mL min^{-1} cm^{-2}. The industrial stream used as the anolyte is stored in a magnetically stirred reservoir, with the temperature held steady at 64 °C using a hot plate.

When using a foam anode, the anodic compartment configuration is adjusted, as depicted in Fig. 1.b. In this setup, the foam is placed in contact with the Nafion 117 membrane, with a Titanium mesh used as the current collector. The foam is integrated into a flow field, allowing the anolyte to pass through its porous structure, thereby maximizing the active area in contact with the electrolyte.

The experiments are carried out at a constant current density of 90 and 200 mA cm^{-2}, provided by a potentiostat-galvanostat (Arbin Instruments, MSTT4). A single liquid sample is collected after each 60-minute experiment, and each experiment is replicated at least twice. Formate concentration in the liquid sample is measured using ion chromatography (Dionex ICS 1100, equipped with an AS9-HC column).

The CO_2 electroreduction performance to formate is evaluated based on the following figures of merit (Eqs. 1–3) [11]:

- Faradaic Efficiency, FE, quantifies the fraction of current density supplied to the electrochemical cell which is utilized for formate production:

$$FE(\%) = \frac{z \bullet M \bullet F}{j \bullet A \bullet t} \times 100 \quad (1)$$

Where z is the number of electrons exchanged in the reduction reaction (2 for formate), M is the number of moles of formate produced during the experimental, F is the Faraday constant (96485 C mol^{-1}), j is the applied current density, A is the electrode's geometric active area, and t is the experimental time.

- Formate rate, r, evaluates the rate of formate production over time and area:

$$r \quad \left(\frac{mmol}{m^2 \quad s}\right) = \frac{M}{t \bullet A} \quad (2)$$

Where M and A are as defined above, and t is the duration of the experiment.

- Energy consumption, EC, measures the total amount of energy required to produce one kilomole of the target product:

$$EC\left(\frac{kWh}{kmol}\right) = \frac{j \bullet A \bullet V \bullet t}{M} \quad (3)$$

Where j, A, t, and M are as defined, and V is the applied potential across the electrolyzer.

3. Results

3.1. Electrocatalyst and electrode characterization

The synthesized electrocatalysts are characterized morphologically and structurally using electron microscopy and X-ray diffraction to confirm their morphology and crystalline structure. Both NiFe and NiZnFe oxides exhibit well-defined and homogeneous shapes (Fig. 2), with their crystalline structures corresponding to a nickel-iron oxide spinel (Figures S1 and S2).

The elemental distribution is consistent across the entire surface, with a homogeneous elemental content on the whole catalyst surface, and the elemental ratios match the initial stoichiometries pre-synthesis. For the decorated Ni foam (NiFe foam), the primary structure is based on the Ni_2P phase, adorned with an amorphous Fe core-shell structure (Figures S3-S9).

In terms of electrochemical properties, the EDLC (electrical double-layer capacitance) shows similar capacitance values for both NiFe and NiZnFe oxides (Figures S13.a and S13.b), with a slight increase for NiZnFe, likely due to the presence of Zn (Figures S10 and S11). The incorporation of Zn may create additional active sites on the catalyst surface in basic media [44].

In contrast, the NiFe foam demonstrates the highest EDLC in the non-faradaic region, as shown in Figure S13.c, with a capacitance of approximately 1.1 mF (Figure S12). This elevated capacitance is attributed to the highly porous surface of the electrode and —dense concentration of actives sites on the material's surface.

For the cathodic electrocatalysts, the TEM images reveal a spherical shape with a narrow particle size distribution, around 9.3 nm [48], as shown in Figure S14. The morphology of the as-prepared GDEs is further investigated by SEM imaging. Top-down SEM and EDX mapping (Figure S15) confirm the uniform distribution of the catalyst on the GDE surface [47,48]. Cross-section analysis determines the GDE thickness, between 275 and 290 μm. Finally, the XRD evaluation (Figure S16) shows that most of the GDE surface is composed of carbon-based materials, with weak Bi-related signals, which is expected since the Bi is supported on carbon in the catalyst nanoparticles [47].

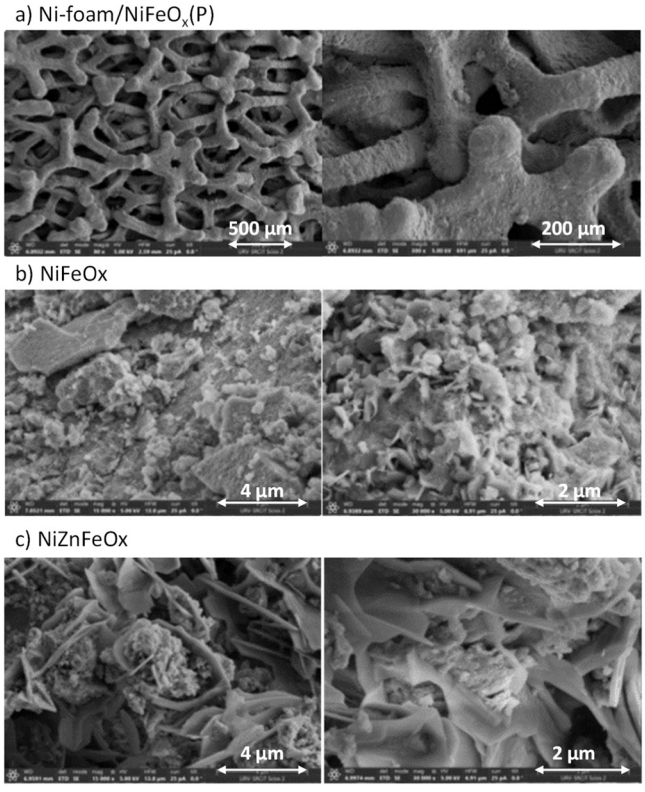

Fig. 2. FESEM images of a) Ni-foam/NiFeOx(P) catalyst, b) NiFeOx, and c) NiZnFeOx.

3.2. Textile industry stream characterization

Samples collected from various stages of the textile industry process are analyzed to evaluate their suitability as anolytes for CO_2 electroreduction. The key parameters evaluated are presented in Table 1:

As shown in Table 1, the temperature of the samples remains consistent at 64 ºC across the textile process. This elevated temperature, significantly above ambient conditions, may influence CO_2 electroreduction performance. Löwe et al. [49] noted that higher temperatures improve GDE system performance due to two main factors: i) they lower cathode potentials at a given current density, improving cathode kinetics and reducing HER impact, and ii) they enhance CO_2 mass transfer through GDE pores due to an increased diffusion coefficient.

pH is another crucial parameter, with all streams being alkaline (pH 10–13). Basic anolytes are commonly employed to suppress HER, maximizing FE for the target product [24]. Additionally, dissolved or suspended solids in the anolytes can lead to the formation of solid deposits on active sites, potentially deactivating the catalyst. Lower solid content in the industrial stream is, therefore, advantageous for maintaining prolonged, stable OER activity on the anode surface. The organic matter content in the textile industry stream is determined utilizing the Chemical Oxygen Demand (COD), with the inlet streams having more concentration, with values ranging from 318 to 438 mg O_2 L^{-1}. The Biological Oxygen Demand (BOD) is not quantified, as the high pH value of the streams might degrade the biodegradable fraction of the organic matter present.

Finally, composition and conductivity are closely linked: higher cation and anion concentrations generally result in increased conductivity, a vital property for efficient anolyte performance as it reduces cell voltage and energy consumption. Streams M1 and C1 exhibit high cation concentrations, particularly Na^+, due to approximately 1.5–2 M NaOH, resulting in high conductivity and ensuring efficient electrochemical cell performance. Conversely, the outlet streams (M2 and C2) show diluted concentrations, resulting in low conductivities (below 50 mS cm^{-1}). As a result, these diluted streams are unsuitable for experimental testing as they do not support efficient CO_2 electrolyzer operation.

3.3. Continuous CO_2 reduction: OER with commercial materials

After characterizing and evaluating the textile industry streams for anolyte suitability, the M1 and C1 streams are selected and used for continuous CO_2 electroreduction to formate using various commercial anode materials: Ir-coated DSA, NiO particulate anode, and Ni foam. The CO_2 electrolyzer's performance is assessed by comparing the behavior of different anode materials and anolytes at two current densities, 90 and 200 mA cm^{-2}. Fig. 3 shows the formate production results for each anode material using both M1 and C1 streams as anolytes.

The different compositions of the two textile industry streams impact the performance of CO_2 electroreduction to formate. As observed in Fig. 3, stream M1, collected from the mercerization process inlet, yields superior performance. When both processes are benchmarked with the DSA, M1 achieves double the formate production compared to C1, underscoring the influence of stream composition. Although C1 has a higher Na^+ concentration and conductivity (Table 1), its efficacy as an anolyte is limited, likely due to its elevated dissolved solids content in C1, which may cause precipitates on catalyst active sites during OER, thereby reducing catalyst activity. Similar trends are observed with NiO PE and Ni Foam anodes. Additionally, the COD at the outlet of the reactor is analyzed for both M1 and C1 streams, with no significant change recorder, thus this confirms that the main oxidation reaction taking place in the anode is the OER.

When assessing the performance of different anode materials with

Table 1
Characterization of textile industry streams for temperature, composition, pH, conductivity, and solid content.

Stream	Temperature (ºC)	Composition (g L^{-1})		pH	Conductivity (mS cm^{-1})	Total solid content (g L^{-1})	Suspended solids (g L^{-1})	COD (mg O_2 L^{-1})
Mercerization inlet (M1)	64 °C	Na^+	35.8	12.05	430	91	3.33	318
		F^-	0.4					
		ClO_2^-	0.4					
		Cl^-	0.6					
		NO_3^-	1					
		SO_2^-	1.8					
		Ca^+	0.3					
		Mg^+	0.4					
Mercerization outlet (M2)	64 °C	Na^+	0.95	12.95	16.75	4.3	0.05	18
		K^+	0.06					
Causticizing inlet (C1)	64 °C	Na^+	45	12.37	547	147.4	0.066	438
		Cl^-	0.01					
		NO_3^-	0.05					
		SO_4^-	0.4					
Causticizing outlet (C2)	64 °C	Na^+	0.329	10.25	1.8	0.81	0.002	62
		Cl^-	0.01					
		NO_3^-	0.16					
		SO_4^-	0.22					
		K^+	0.02					

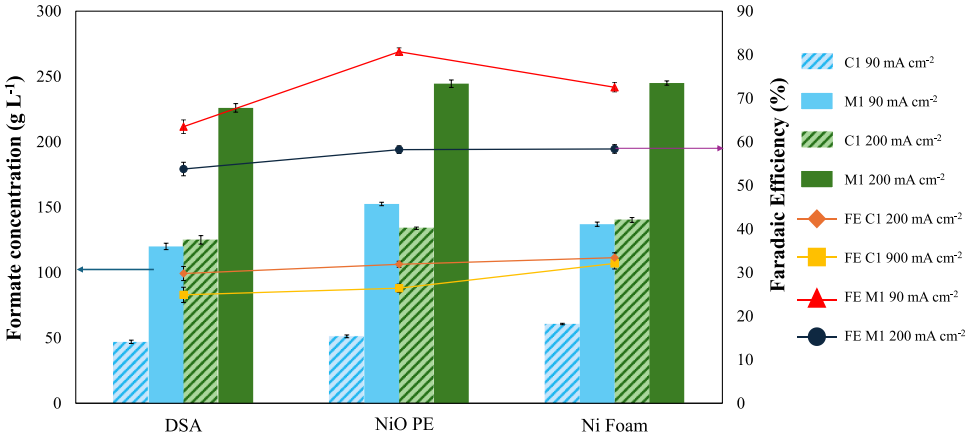

Fig. 3. Formate concentration and FE results for continuous CO_2 electroreduction to formate in the gas phase using different anode materials and analyte compositions (Textile industry streams M1 and C1).

the M1 stream (the better-performing analyte), we observe variations in formate production. With the DSA, formate concentrations of 120 and 226 g L^{-1} are obtained for 90 and 200 mA cm^{-2}, respectively, with FEs of 63 and 53 %. Compared to previous works by Diaz-Sainz et al. [12], the formate concentration is lower, but the FE is slightly higher. However, the shift from K^+ to Na^+ in the anolyte may have affected cathode

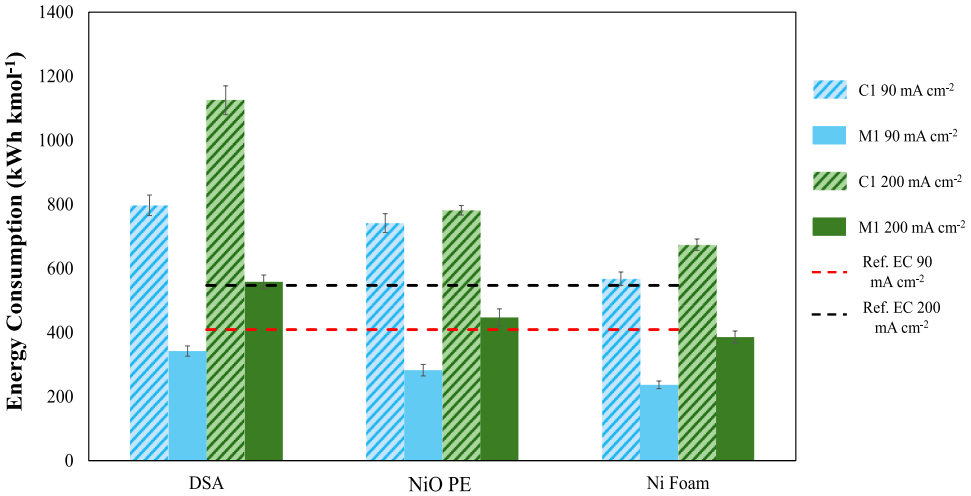

Fig. 4. Energy consumption results for DSA plate, NiO PE, and Ni Foam, using M1 and C1 streams as anolytes, compared to previous results with DSA and 1 M KOH [12].

performance, as the formation of less soluble Na-salts can alter the GDE structure during CO_2 electrolysis [26,50]. Despite this, DSA underperformed for CO_2 electroreduction to formate, with NiO PE and Ni foam showing 15–22 and 10 % higher formate production at 90 and 200 mA cm^{-2}, respectively, largely due to the higher electrochemical surface area compared to the DSA plate [38,51].

Among the anodes, NiO PE shows the highest formate production, reaching concentrations of 153 and 244 g L^{-1} at 90 and 200 mA cm^{-2}, with FEs of 80.5 and 58.5 %, respectively. This outperforms Ni foam, especially at 90 mA cm^{-2}, where formate production is 10 % lower (139 g L^{-1} with 72 % FE). At 200 mA cm^{-2}, both anodes show similar CO_2 conversion, with formate concentrations of 245 g L^{-1} and 58.5 % of FE. Both anodes produced comparable formate rates at high current densities, around 6.03 mmol m^{-2} s^{-1}.

Another crucial factor is the system's energy consumption, essential for evaluating industrial scalability. Energy consumption results are compared in Fig. 4 with previous work using a DSA with synthetic 1 M KOH as the anolyte [12]:

As with formate production, the C1 stream produces poorer results than M1, with higher cell voltages and lower formate production, resulting in increased energy consumption. This further indicates the unsuitability of C1 as an anolyte for continuous CO_2 electroreduction to formate. On the other hand, M1 shows excellent performance across all anode materials, with reduced energy consumption compared to synthetic 1 M KOH. This demonstrates the potential of coupling textile industry stream oxidation to lower energy requirements and enhances the competitive viability of this technology competitively for future industrial implementation.

Of the anode materials, Ni foam exhibited the lowest energy consumption due to a significant reduction in cell potential, from 5.6 to 4.7 V when compared to the DSA, working at 200 mA cm^{-2}. This is attributed to its three-dimensional structure, allowing the formation of a zero-gap anode where the anode material is in direct contact with the ion exchange membrane while the anolyte flows through its pores [52]. Ni foam's energy consumption is 236 and 385 kWh $kmol^{-1}$ at 90 and 200 mA cm^{-2}, respectively. Compared to previous studies, this represents a 43 and 30 % reduction in energy consumption, bringing it closer to the target value of 238 kWh $kmol^{-1}$ at current densities above 200 mA cm^{-2} [53].

3.4. *$ERCO_2$ coupling with alternative anode material for OER using textile industry streams*

The mercerization inlet stream, M1, having demonstrated the best performance in previous analyses, is selected as the anolyte for testing synthesized Ni-based anodes. These materials aim to assess the use of abundant catalysts for the OER under industrial conditions coupled with CO_2 electroreduction to formate. Performance results for CO_2 conversion to formate are presented in Fig. 5.

The NiZnFeOx particulate anode and NiFe foam demonstrate similar results, achieving formate concentrations of approximately 140 and 250 g L^{-1} for 90 and 200 mA cm^{-2}, respectively, equivalent to commercial NiOx and Ni foam electrodes (Fig. 5). This result underscores the potential for coupling synthesized Ni-based materials with CO_2 electroreduction. On the other hand, the NiFeOx anode shows lower formate production, with concentrations between 95 and 170 g L^{-1} at 90 and 200 mA cm^{-2}. This reduced performance can be attributed to its lower EDLC compared to NiZnFeOx, as presented in Figure S13. The addition of Zn in NiZnFeOx increases EDLC, which enhances OER kinetics, improves charge transfer to the cathode, and boosts CO_2 reduction performance [54]. In this case, Zn serves as a sacrificial material during the electrolysis. Due to the solubility of Zn in alkaline media, it dissolves, exposing fresh active sites for OER and directly improving the EDCL. This suggests that Zn leaching is only partial, likely originating from significant defects or specific crystal facets, within the oxide structure. This leaching may be associated with the observed EDCL enhancement under working conditions, as ion leaching could increase the material's surface area, thereby improving the accessibility of active sites for water molecules. In terms of FE, the NiZnFeOx and NiFe foam anodes also yield competitive results for CO_2 gas-phase conversion, with FEs around 75 % at 90 mA cm^{-2} and 60 % at 200 mA cm^{-2}. Formate production rates reach approximately 3.45 and 6.4 mmol m^{-2} s^{-1} for NiFe foam at 90 and 200 mA cm^{-2}, respectively representing improved CO_2 reduction kinetics compared to commercial anodes, due to greater electron availability at the cathode.

The possible degradation of the synthesized anodic materials on the industrial effluent under oxidation conditions is addressed. Despite the alkalinity of the M1 stream, the presence of Cl^- might raise concerns, as the electrochemical Cl^- oxidation could result in inefficient OER and even cause corrosion of the anode material. To evaluate this, the outlet of the anolyte compartment is evaluated to assess any change in the Cl^- during the single pass through the electrochemical reactor. No significative alteration in the Cl^- concentration is observed, which remained around 0.6 g L^{-1}, indicating that Cl^- is not oxidized. Moreover, as the Cl^- concentration is relatively low, no degradation of the anodic materials occurred after the experimentation, confirming the stability of the materials during the $ERCO_2$ tests.

An essential parameter in evaluating the potential of different anode materials is the anodic overpotential, which often represents a significant portion of the external energy needed for CO_2 electroreduction. Changes in overpotential are reflected in the energy consumption for producing formate. Energy consumption results for the synthesized

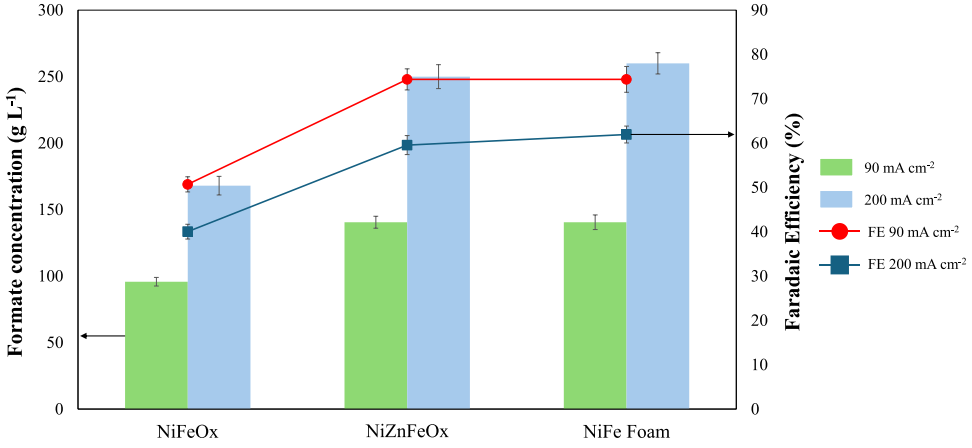

Fig. 5. Formate concentration and FE results for coupling CO_2 electroreduction to formate in the gas phase using synthesized NiFeOx, NiZnFeOX, and NiFe Foam anodes.

different materials are depicted in Fig. 6:

A clear trend emerges in line with EDLC results: lower Capacitance Double Layer (Cdl) values correspond to higher energy consumption. Consequently, the NiFeOx particulate anode, with a Cdl of $4{\cdot}10^{-3}$ mF, shows the highest energy consumptions, at 545 and 926 kWh kmol^{-1} for 90 and 200 mA cm^{-2}, respectively. The NiZnFeOx particulate anode improves the energy consumption by 10–20 %, reducing requirements to 490 and 790 kWh kmol^{-1} for 90 and 200 mA cm^{-2}, respectively. The NiFe foam anode provides the most substantial energy reduction, thanks to its three-dimensional structure and anolyte flow-through design. This structure offers a larger active surface area, which accesses numerous active sites for OER, while the high EDLC (1.1 mF) enhances charge storage on the active surface area [55]. This improved accessibility of charged species enables both OER and CO_2 reduction, while the large interface area between the anolyte and the anode material enhances the OER kinetics by minimizing mass transfer limitations [56]. Moreover, the well-developed double layer facilitates charge transport, reducing anode overpotential, resulting in a 4.4 V cell potential, and resulting in remarkably low energy consumptions for gas-phase CO_2 electroreduction to formate (209 and 380 kWh kmol^{-1} at 90 and 200 mA cm^{-2}). Compared to results with a commercial Ni foam, these findings show that electrodeposition of an additional Ni-Fe catalyst can further reduce energy requirements by up to 10 %.

Gas-phase CO_2 electroreduction to formate, using a humidified CO_2 stream as the sole feed to the cathode, has garnered significant attention in recent years. Most studies have employed synthetic anolytes to facilitate the OER at the anode. Table 2 presents a comparison of the key figures of merit from previous studies alongside the results of the present work.

The obtained FE and energy consumption fall within the range of previously reported values, achieving one of the best trade-offs between formate concentration, FE, and energy consumption at a current density of 200 mA cm^{-2}.

This work demonstrates the potential of coupling industrial stream oxidation with CO_2 electroreduction to formate, achieving high conversion efficiency for both commercial and synthesized anode materials. Additionally, using textile industry streams shows potential for significantly lowering energy consumption at high current densities. Particularly promising results are obtained with foam-type anodes, reaching the target 4.3 V of cell overall potential at current densities exceeding 200 mA cm^{-2} [53], to make the CO_2 electroreduction to formate process economically feasible.

4. Conclusions

The scale-up of CO_2 electroreduction to formate faces several challenges, particularly due to the use of chemicals as anolytes and the need to reduce energy demands for economic feasibility at an industrial scale. To address these challenges, this study uses textile industry streams as anolytes for the OER. Promising results are obtained using a highly concentrated caustic soda stream, sourced from the inlet of the mercerization process in a textile industry. Formate concentrations of 226 g L^{-1} with a FE of 53 % are reached at 200 mA cm^{-2} using a DSA plate, showing better FE performance than previous trials with synthetic 1 M KOH anolyte solutions. This result highlights the potential for combining the oxidation of textile industry streams with industrially relevant conditions to scale up CO_2 electroreduction to formate.

The study also evaluates different anode materials to enhance the OER kinetics, improve CO_2 electroreduction efficiency, and reduce overall energy consumption. Two different approaches were proposed: using commercially available anode materials and developing new, cost-effective materials. In the first approach, a DSA anode, a NiO particulate anode, and a Ni foam are compared. Both the NiO and Ni foam anodes achieve excellent formate concentrations of approximately 150 and 245 g L^{-1}, with FEs of 78 and 58 % at 90 and 200 mA cm^{-2}, respectively. Ni foam also significantly reduces energy consumption to 236 and 385 kWh kmol^{-1}, benefiting from its high surface area provided by its three-dimensional structure.

The second approach involves synthesizing alternative anode materials from abundant elements to reduce the cost of OER catalysts. Here, NiFeOx and NiZnFeOx particulate anodes, as well as NiFe foam, are employed using the mercerization inlet stream as the anolyte. NiZnFeOx and NiFe foam achieve high formate concentrations of 140 and 255 g L^{-1}, with FEs of 74 and 60 % at 90 and 200 mA cm^{-2}, respectively, showing comparable performance to commercial NiO and Ni foam. Notably, NiFe foam demonstrates the lowest energy consumption, attributed to its high ECDL and improved charge transfer due to its large active surface area. NiFe foam achieves energy consumption values under 210 and 380 kWh kmol^{-1}, surpassing commercial Ni foam. Additionally, a reduced cell potential of 4.4 V is achieved at 200 mA cm^{-2}, nearing the target of 4.3 V required for economic scalability at an industrial level.

All in all, this work successfully demonstrates the feasibility of CO_2 electroreduction to formate using textile industry streams as anolytes obtaining outstanding formate production and reduced energy consumption. This represents a significant advancement toward establishing CO_2 electroreduction to formate as a viable solution for the decarbonization of hard-to-abate industries.

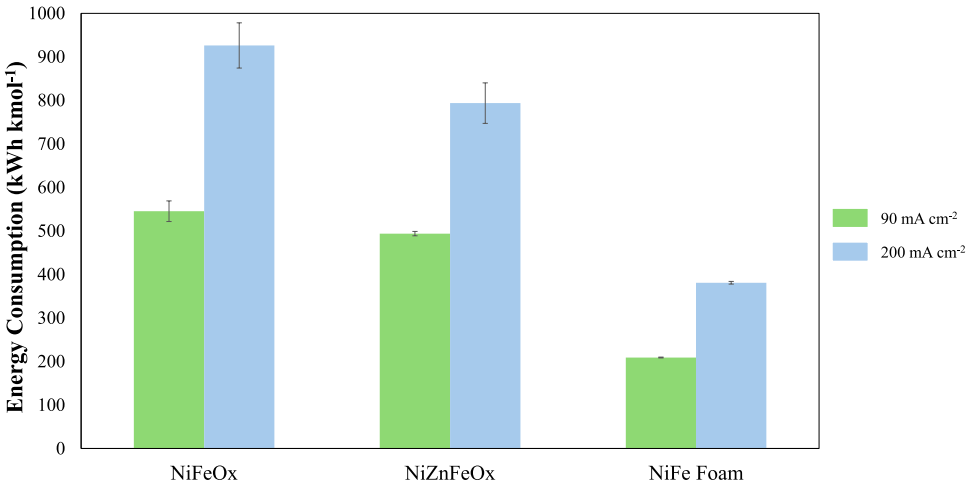

Fig. 6. Energy consumption results from coupling the alternative anode materials with CO_2 electroreduction to formate in gas phase.

Table 2
Main figures of merit for the $ERCO_2$ to formate reported in the literature, compared to the results of the present work.

Cathode	Anode	Anolyte	[$HCOO^-$] (g L^{-1})	j (mA cm^{-2})	FE (%)	EC (kWh $kmol^{-1}$)	[Ref.]
Sn	Pt/C	1 M KOH	116.0	40	78	152	[57]
Sn	DSA	1 M KOH	19.2	45	49	244	[58]
Sn	Ni Foam	2 M KOH	65.4	100	80	181	[59]
Bi	DSA	1 M KOH	43.2	200	43	434	[60]
Bi	DSA	1 M KOH	337.0	45	89	180	[12]
Bi	DSA	1 M KOH	312.0	200	25	547	[12]
Bi	DSA	1 M KOH	10.8	600	74	342	[61]
Bi-Sn	IrO_x on Ti Foam	0.1 M $KHCO_3$	153.0	60	82	267	[62]
Bi-Sn	IrO_2 on Ti Foam	0.1 M $KHCO_3$	0.36	120	80	268	[63]
Bi	DSA	0.3 M K_2SO_4 (pH 1)	88.0	200	42	358	[26]
Bi	$CaTiO_3$-$BiVO_4$	0.5 M $KHCO_3$	63.8	32	79	318	[64]
Bi	Ni-Co Foam	1 M KOH + 1 M glycerol	359.0	45	95	192	[52]
Bi	NiFe Foam	Textile industry stream (NaOH)	260.0	200	62	380	[This work]

CRediT authorship contribution statement

Abarca Jose Antonio: Writing – original draft, Validation, Methodology, Investigation, Data curation, Conceptualization. **Garcés-Pineda Felipe A.:** Writing – review & editing, Validation, Supervision, Methodology, Investigation. **Solla-Gullon Jose:** Writing – review & editing, Project administration, Funding acquisition. **Abdolhosseini Ghazaleh:** Validation, Methodology, Investigation. **Sanz Juan Marcos:** Project administration, Methodology, Investigation, Funding acquisition. **Díaz-Sainz Guillermo:** Writing – review & editing, Writing – original draft, Supervision, Methodology, Investigation, Data curation, Conceptualization. **Irabien Angel:** Writing – review & editing, Supervision, Project administration, Funding acquisition.

Declaration of Competing Interest

The authors declare that they have no known competing financial interests or personal relationships that could have appeared to influence the work reported in this paper.

Acknowledgements

The authors gratefully acknowledge Grant TED2021-129810B-C21 and PLEC2022-009398 funded by MICIU/AEI/10.13039/501100011033/ and by the "European Union NextGenerationEU/PRTR", and Grants PID2022-138491OB-C31, and PID2022-138491OB-C32, funded by MICIU/AEI/10.13039/501100011033 and by "ERDF/EU". The present work is related to CAPTUS Project. This project has received funding from the European Union's Horizon Europe research and innovation programme under grant agreement No 101118265. J. A. Abarca gratefully acknowledges the predoctoral research grant (FPI) PRE2021-097200.

Appendix A. Supporting information

Supplementary data associated with this article can be found in the online version at doi:10.1016/j.jcou.2025.103053.

Data availability

Data will be made available on request.

References

[1] Global Greenhouse Gas Overview | US EPA. ⟨https://www.epa.gov/ghgemissions/global-greenhouse-gas-overview⟩ (accessed November 29, 2024).
[2] COP28 - NET-ZERO TRANSITION CHARTER. ⟨https://www.cop28.com/en/net-zero-accountability-charter⟩ (accessed November 29, 2024).
[3] S. Fawzy, A.I. Osman, J. Doran, D.W. Rooney, Strategies for mitigation of climate change: a review, Environ. Chem. Lett. 18 (2020) 2069–2094, https://doi.org/10.1007/S10311-020-01059-W.
[4] A.I. Osman, M. Hefny, M.I.A. Abdel Maksoud, A.M. Elgarahy, D.W. Rooney, Recent advances in carbon capture storage and utilisation technologies: a review, Environ. Chem. Lett. 19 (2021) 797–849, https://doi.org/10.1007/s10311-020-01133-3.
[5] R. Fiorenza, L. Calantropo, E. La Greca, L.F. Liotta, A. Gulino, A. Ferlazzo, M. G. Musumeci, G. Proietto Salanitri, S.C. Carroccio, G. Dativo, M.T. Armeli Iapichino, S. Scirè, G. Impellizzeri, Solar-promoted photo-thermal CO_2 methanation on SiC/hydrotalcites-derived catalysts, Catal. Today 449 (2025) 115182, https://doi.org/10.1016/J.CATTOD.2024.115182.
[6] D. Xu, K. Li, B. Jia, W. Sun, W. Zhang, X. Liu, T. Ma, Electrocatalytic CO_2 reduction towards industrial applications, Carbon Energy 5 (2023) e230, https://doi.org/10.1002/cey2.230.
[7] Y.Y. Birdja, E. Pérez-Gallent, M.C. Figueiredo, A.J. Göttle, F. Calle-Vallejo, M.T. M. Koper, Advances and challenges in understanding the electrocatalytic conversion of carbon dioxide to fuels, Nat. Energy 4 (2019) 732–745, https://doi.org/10.1038/s41560-019-0450-y.
[8] J. Antonio Abarca, G. Díaz-Sainz, I. Merino-Garcia, A. Irabien, J. Albo, Photoelectrochemical CO_2 electrolyzers: from photoelectrode fabrication to reactor configuration, J. Energy Chem. 85 (2023) 455–480, https://doi.org/10.1016/j.jechem.2023.06.032.
[9] M.S. Kim, A. Priyadarsini, J.H. Lee, J.G. Bae, J.Y. Heo, H.J. Lee, S. Kattel, J.H. Lee, Ligand environment engineering of nickel single atomic sites for efficient electrochemical carbon dioxide reduction reaction, J. Mater. Chem. A Mater. 13 (2025) 3834–3848, https://doi.org/10.1039/D4TA06720G.
[10] J. Sheng, M. Gao, N. Zhao, K. Zhao, Y. Shi, W. Wang, Bimetallic Ni/Fe functionalized, 3D printed, self-supporting catalytic-electrodes for CO_2 reduction reaction, Fuel 382 (2025) 133703, https://doi.org/10.1016/J.FUEL.2024.133703.
[11] K. Fernández-Caso, G. Díaz-Sainz, M. Alvarez-Guerra, A. Irabien, Electroreduction of CO_2: advances in the continuous production of formic acid and formate, ACS Energy Lett. 8 (2023) 1992–2024, https://doi.org/10.1021/ACSENERGYLETT.3C00489.
[12] G. Díaz-Sainz, M. Alvarez-Guerra, B. Ávila-Bolívar, J. Solla-Gullón, V. Montiel, A. Irabien, Improving trade-offs in the figures of merit of gas-phase single-pass continuous CO_2 electrocatalytic reduction to formate, Chem. Eng. J. 405 (2021) 126965, https://doi.org/10.1016/J.CEJ.2020.126965.
[13] T. Moore, X. Xia, S.E. Baker, E.B. Duoss, V.A. Beck, Elucidating mass transport regimes in gas diffusion electrodes for CO_2electroreduction, ACS Energy Lett. 6 (2021) 3600–3606, https://doi.org/10.1021/acsenergylett.1c01513.
[14] I. Merino-Garcia, E. Alvarez-Guerra, J. Albo, A. Irabien, Electrochemical membrane reactors for the utilisation of carbon dioxide, Chem. Eng. J. 305 (2016) 104–120, https://doi.org/10.1016/J.CEJ.2016.05.032.
[15] J. Park, Y. jin Ko, C. Lim, H. Kim, B.K. Min, K.Y. Lee, J.H. Koh, H.S. Oh, W.H. Lee, Strategies for CO_2 electroreduction in cation exchange membrane electrode assembly, Chem. Eng. J. 453 (2023) 139826, https://doi.org/10.1016/j.cej.2022.139826.
[16] M. Bevilacqua, J. Filippi, A. Lavacchi, A. Marchionni, H.A. Miller, W. Oberhauser, E. Vesselli, F. Vizza, M. Bevilacqua, J. Filippi, A. Lavacchi, A. Marchionni, H. A. Miller, W. Oberhauser, F. Vizza, E. Vesselli, Energy savings in the conversion of CO_2 to fuels using an electrolytic device, Energy Tech. 2 (2014) 522–525, https://doi.org/10.1002/ENTE.201402014.
[17] D. Wu, J. Hao, Z. Song, X.Z. Fu, J.L. Luo, All roads lead to Rome: an energy-saving integrated electrocatalytic CO_2 reduction system for concurrent value-added formate production, Chem. Eng. J. 412 (2021) 127893, https://doi.org/10.1016/J.CEJ.2020.127893.
[18] Y. Zhang, J. Lan, F. Xie, M. Peng, J. Liu, T.S. Chan, Y. Tan, Aligned InS nanorods for efficient electrocatalytic carbon dioxide reduction, ACS Appl. Mater. Interfaces 14 (2022) 25257–25266, https://doi.org/10.1021/ACSAMI.2C01152.
[19] S. Sabatino, A. Galia, G. Saracco, O. Scialdone, Development of an electrochemical process for the simultaneous treatment of wastewater and the conversion of carbon dioxide to higher value products, ChemElectroChem 4 (2017) 150–159, https://doi.org/10.1002/CELC.201600475.
[20] Q. Wang, X. Wang, C. Wu, Y. Cheng, Q. Sun, H. Yu, Enhanced electroreduction of CO_2 and simultaneous degradation of organic pollutants using a Sn-based carbon nanotubes/carbon black hybrid gas diffusion cathode, J. CO_2 Util. 26 (2018) 425–433, https://doi.org/10.1016/j.jcou.2018.05.027.

[21] K. Fernández-Caso, A. Peña-Rodríguez, J. Solla-Gullón, V. Montiel, G. Díaz-Sainz, M. Alvarez-Guerra, A. Irabien, Continuous carbon dioxide electroreduction to formate coupled with the single-pass glycerol oxidation to high value-added products, J. CO_2 Util. 70 (2023) 102431, https://doi.org/10.1016/j.jcou.2023.102431.

[22] S. Verma, S. Lu, P.J.A. Kenis, Co-electrolysis of CO_2 and glycerol as a pathway to carbon chemicals with improved technoeconomics due to low electricity consumption, Nat. Energy 4 (2019) 466–474, https://doi.org/10.1038/s41560-019-0374-6.

[23] W. Xie, B. Li, L. Liu, H. Li, M. Yue, Q. Niu, S. Liang, X. Shao, H. Lee, J.Y. Lee, M. Shao, Q. Wang, D. O'Hare, H. He, Advanced systems for enhanced CO_2 electroreduction, Chem. Soc. Rev. 54 (2025) 898–959, https://doi.org/10.1039/d4cs00563e.

[24] C.P. O'Brien, R.K. Miao, S. Liu, Y. Xu, G. Lee, A. Robb, J.E. Huang, K. Xie, K. Bertens, C.M. Gabardo, J.P. Edwards, C.T. Dinh, E.H. Sargent, D. Sinton, Single Pass CO2Conversion Exceeding 85% in the Electrosynthesis of Multicarbon Products via Local CO_2Regeneration, ACS Energy Lett. 6 (2021) 2952–2959, https://doi.org/10.1021/ACSENERGYLETT.1C01122.

[25] E.R. Cofell, U.O. Nwabara, S.S. Bhargava, D.E. Henckel, P.J.A. Kenis, Investigation of electrolyte-dependent carbonate formation on gas diffusion electrodes for CO2electrolysis, ACS Appl. Mater. Interfaces 13 (2021) 15132–15142, https://doi.org/10.1021/ACSAMI.0C21997.

[26] J.A. Abarca, G. Díaz-Sainz, A. Irabien, Inhibiting salt precipitation on the gas diffusion electrode surface in gas-phase CO_2 electroreduction to formate by using an acidic anolyte, J. CO_2 Util. 86 (2024) 102897, https://doi.org/10.1016/J.JCOU.2024.102897.

[27] Vass, B. Endrődi, C. Janáky, Coupling electrochemical carbon dioxide conversion with value-added anode processes: an emerging paradigm, Curr. Opin. Electrochem 25 (2021) 100621, https://doi.org/10.1016/j.coelec.2020.08.003.

[28] Y. Cheng, P. Hou, X. Wang, P. Kang, CO_2 Electrolysis system under industrially relevant conditions, Acc. Chem. Res. 55 (2022) 231–240, https://doi.org/10.1021/acs.accounts.1c00614.

[29] K. Niinimäki, G. Peters, H. Dahlbo, P. Perry, T. Rissanen, A. Gwilt, The environmental price of fast fashion, Nat. Rev. Earth Environ. 1 (2020) 189–200, https://doi.org/10.1038/s43017-020-0039-9.

[30] C.R. Holkar, A.J. Jadhav, D.V. Pinjari, N.M. Mahamuni, A.B. Pandit, A critical review on textile wastewater treatments: Possible approaches, J. Environ. Manag. 182 (2016) 351–366, https://doi.org/10.1016/j.jenvman.2016.07.090.

[31] G.A. Kallawar, B.A. Bhanvase, A review on existing and emerging approaches for textile wastewater treatments: challenges and future perspectives, Environ. Sci. Pollut. Res. 31 (2023) 1748–1789, https://doi.org/10.1007/s11356-023-31175-3.

[32] M. Balkan, E. Ozturk, M. Kitis, Economic and cross-media effect analyses of best available techniques for caustic recovery from mercerization textile wastewater, Clean. Technol. Environ. Policy 25 (2023) 1043–1058, https://doi.org/10.1007/s10098-022-02424-9.

[33] G. Díaz-Sainz, J.A. Abarca, M. Alvarez-Guerra, A. Irabien, Exploring the impact of partial pressure and typical compounds on the continuous electroconversion of CO_2 into formate, J. CO_2 Util. 81 (2024) 102735, https://doi.org/10.1016/j.jcou.2024.102735.

[34] J. Wang, Y. Gao, H. Kong, J. Kim, S. Choi, F. Ciucci, Y. Hao, S. Yang, Z. Shao, J. Lim, Non-precious-metal catalysts for alkaline water electrolysis: operando characterizations, theoretical calculations, and recent advances, Chem. Soc. Rev. 49 (2020) 9154–9196, https://doi.org/10.1039/d0cs00575d.

[35] H. Zhou, F. Yu, J. Sun, R. He, S. Chen, C.W. Chu, Z. Ren, Highly active catalyst derived from a 3D foam of Fe(PO3)2/Ni2P for extremely efficient water oxidation, Proc. Natl. Acad. Sci. 114 (2017) 5607–5611, https://doi.org/10.1073/pnas.1701562114.

[36] A. Löwe, M. Schmidt, F. Bienen, D. Kopljar, N. Wagner, E. Klemm, Optimizing reaction conditions and gas diffusion electrodes applied in the CO_2reduction reaction to formate to reach current densities up to 1.8 A cm^{-2}, ACS Sustain. Chem. Eng. 9 (2021) 4213–4223, https://doi.org/10.1021/ACSSUSCHEMENG.1C00199.

[37] J. Zou, C.Y. Lee, G.G. Wallace, A non-noble metal catalyst-based electrolyzer for efficient CO_2-to-formate conversion, ACS Sustain. Chem. Eng. 9 (2021) 16394–16402, https://doi.org/10.1021/ACSSUSCHEMENG.1C06295.

[38] G. Díaz-Sainz, K. Fernández-Caso, T. Lagarteira, S. Delgado, M. Alvarez-Guerra, A. Mendes, A. Irabien, Coupling continuous CO_2electroreduction to formate with efficient Ni-based anodes, J. Environ. Chem. Eng. 11 (2023) 109171, https://doi.org/10.1016/j.jece.2022.109171.

[39] J.D. Holladay, J. Hu, D.L. King, Y. Wang, An overview of hydrogen production technologies, Catal. Today 139 (2009) 244–260, https://doi.org/10.1016/j.cattod.2008.08.039.

[40] T. Fan, W. Ma, M. Xie, H. Liu, J. Zhang, S. Yang, P. Huang, Y. Dong, Z. Chen, X. Yi, Achieving high current density for electrocatalytic reduction of CO_2 to formate on bismuth-based catalysts, Cell. Rep. Phys. Sci. 2 (2021) 100353, https://doi.org/10.1016/J.XCRP.2021.100353.

[41] Z.F. Huang, J. Wang, Y. Peng, C.Y. Jung, A. Fisher, X. Wang, Design of efficient bifunctional oxygen reduction/evolution electrocatalyst: recent advances and perspectives, Adv. Energy Mater. 7 (2017) 1700544, https://doi.org/10.1002/aenm.201700544.

[42] Y. Zhou, N. López, The role of Fe species on NiOOH in oxygen evolution reactions, ACS Catal. 10 (2020) 6254–6261, https://doi.org/10.1021/acscatal.0c00304.

[43] L. Trotochaud, S.L. Young, J.K. Ranney, S.W. Boettcher, Nickel-Iron oxyhydroxide oxygen-evolution electrocatalysts: the role of intentional and incidental iron incorporation, J. Am. Chem. Soc. 136 (2014) 6744–6753, https://doi.org/10.1021/ja502379c.

[44] H.C. Nguyën, F.A. Garcés-Pineda, M. De Fez-Febré, J.R. Galán-Mascarós, N. López, Non-redox doping boosts oxygen evolution electrocatalysis on hematite, Chem. Sci. 11 (2020) 2464–2471, https://doi.org/10.1039/c9sc05669f.

[45] F.A. Garcés-Pineda, H. Chuong Nguyën, M. Blasco-Ahicart, M. García-Tecedor, M. de Fez Febré, P.Y. Tang, J. Arbiol, S. Giménez, J.R. Galán-Mascarós, N. López, Push-pull electronic effects in surface-active sites enhance electrocatalytic oxygen evolution on transition metal oxides, ChemSusChem 14 (2021) 1595–1601, https://doi.org/10.1002/cssc.202002782.

[46] J. Roth, B. Zerger, D. De Geeter, J. Gómez Benavides, S. Roudier, Best available techniques (BAT) reference document for the Textiles Industry, (2023). https://doi.org/10.2760/355887.

[47] J.A. Abarca, G. Díaz-Sainz, I. Merino-Garcia, G. Beobide, J. Albo, A. Irabien, Optimized manufacturing of gas diffusion electrodes for CO_2 electroreduction with automatic spray pyrolysis, J. Environ. Chem. Eng. (2023) 109724, https://doi.org/10.1016/J.JECE.2023.109724.

[48] G. Díaz-Sainz, M. Alvarez-Guerra, J. Solla-Gullón, L. García-Cruz, V. Montiel, A. Irabien, CO2 electroreduction to formate: continuous single-pass operation in a filter-press reactor at high current densities using Bi gas diffusion electrodes, J. CO_2 Util. 34 (2019) 12–19, https://doi.org/10.1016/J.JCOU.2019.05.035.

[49] A. Löwe, C. Rieg, T. Hierlemann, N. Salas, D. Kopljar, N. Wagner, E. Klemm, Influence of temperature on the performance of gas diffusion electrodes in the CO_2 reduction reaction, ChemElectroChem 6 (2019) 4497–4506, https://doi.org/10.1002/celc.201900872.

[50] J. Disch, L. Bohn, L. Metzler, S. Vierrath, Strategies for the mitigation of salt precipitation in zero-gap CO_2 electrolyzers producing CO, J. Mater. Chem. A Mater. 11 (2023) 7344–7357, https://doi.org/10.1039/d2ta09966g.

[51] W. Zhu, R. Zhang, F. Qu, A.M. Asiri, X. Sun, Design and application of foams for electrocatalysis, ChemCatChem 9 (2017) 1721–1743, https://doi.org/10.1002/cctc.201601607.

[52] K. Fernández-Caso, M. Molera, T. Andreu, J. Solla-Gullón, V. Montiel, G. Díaz-Sainz, M. Álvarez-Guerra, A. Irabien, Coupling glycerol oxidation reaction using Ni-Co foam anodes to CO_2 electroreduction in gas-phase for continuous co-valorization, Chem. Eng. J. 480 (2024) 147908, https://doi.org/10.1016/J.CEJ.2023.147908.

[53] M. Rumayor, A. Dominguez-Ramos, P. Perez, A. Irabien, A techno-economic evaluation approach to the electrochemical reduction of CO_2 for formic acid manufacture, J. CO_2 Util. 34 (2019) 490–499, https://doi.org/10.1016/J.JCOU.2019.07.024.

[54] X. Zhao, L. Du, B. You, Y. Sun, Integrated design for electrocatalytic carbon dioxide reduction, Catal. Sci. Technol. 10 (2020) 2711–2720, https://doi.org/10.1039/d0cy00453g.

[55] M. Dunwell, Y. Yan, B. Xu, H.C. Zeng, H. Yang, Understanding the influence of the electrochemical double-layer on heterogeneous electrochemical reactions, Curr. Opin. Chem. Eng. 20 (2018) 151–158, https://doi.org/10.1016/j.coche.2018.05.003.

[56] G. Li, L. Anderson, Y. Chen, M. Pan, P.Y. Abel Chuang, New insights into evaluating catalyst activity and stability for oxygen evolution reactions in alkaline media, Sustain. Energy Fuels. 2 (2017) 237–251, https://doi.org/10.1039/C7SE00337D.

[57] W. Lee, Y. Oung, E. Kim, M.H. Youn, S.K. Jeong, K. Taep, Catholyte-free electrocatalytic CO_2 reduction to formate, Angew. Chem. 130 (2018) 6999–7003, https://doi.org/10.1002/ANGE.201803501.

[58] G. Díaz-Sainz, M. Alvarez-Guerra, J. Solla-Gullón, L. García-Cruz, V. Montiel, A. Irabien, Catalyst coated membrane electrodes for the gas phase CO_2 electroreduction to formate, Catal. Today 346 (2020) 58–64, https://doi.org/10.1016/J.CATTOD.2018.11.073.

[59] B. De Mot, M. Ramdin, J. Hereijgers, T.J.H. Vlugt, T. Breugelmans, Direct water injection in catholyte-free zero-gap carbon dioxide electrolyzers, ChemElectroChem 7 (2020) 3839–3843, https://doi.org/10.1002/CELC.202000961.

[60] G. Díaz-Sainz, M. Alvarez-Guerra, J. Solla-Gullón, L. García-Cruz, V. Montiel, A. Irabien, Gas–liquid–solid reaction system for CO_2 electroreduction to formate without using supporting electrolyte, AIChE J. 66 (2020) e16299, https://doi.org/10.1002/AIC.16299.

[61] G. Díaz-Sainz, M. Alvarez-Guerra, A. Irabien, Continuous electroreduction of CO_2 towards formate in gas-phase operation at high current densities with an anion exchange membrane, J. CO_2 Util. 56 (2022) 101822, https://doi.org/10.1016/J.JCOU.2021.101822.

[62] L. Li, A. Ozden, S. Guo, F.P. García de Arquer, C. Wang, M. Zhang, J. Zhang, H. Jiang, W. Wang, H. Dong, D. Sinton, E.H. Sargent, M. Zhong, Stable, active CO_2 reduction to formate via redox-modulated stabilization of active sites, Nat. Comm. 12 (2021) 1–9, https://doi.org/10.1038/s41467-021-25573-9.

[63] K. Yao, H. Wang, X. Yang, Y. Huang, C. Kou, T. Jing, S. Chen, Z. Wang, Y. Liu, H. Liang, Metal-organic framework derived dual-metal sites for electroreduction of carbon dioxide to HCOOH, Appl. Catal. B 311 (2022) 121377, https://doi.org/10.1016/J.APCATB.2022.121377.

[64] J.A. Abarca, I. Merino-Garcia, G. Díaz-Sainz, M. Perfecto-Irigaray, G. Beobide, A. Irabien, J. Albo, Fabrication and optimization of perovskite-based photoanodes for solar-driven CO_2 photoelectroreduction to formate, Catal. Today 429 (2024) 114505, https://doi.org/10.1016/j.cattod.2023.114505.